

# Mathematical modeling of bulk and directional crystallization with the moving phase transition layer

Liubov V. Toropova<sup>1,2</sup>  | Danil L. Aseev<sup>2</sup>  | Sergei I. Osipov<sup>2</sup> | Alexander A. Ivanov<sup>2</sup> 

<sup>1</sup>Otto-Schott-Institut für Materialforschung, Friedrich Schiller Universität Jena, Jena, Germany

<sup>2</sup>Laboratory of Multi-Scale Mathematical Modeling, Institute of Natural Sciences and Mathematics, Ural Federal University, Ekaterinburg, Russian Federation

## Correspondence

Liubov V. Toropova, Otto-Schott-Institut für Materialforschung, Friedrich Schiller Universität Jena, 07743 Jena, Germany.  
Email: liubov.toropova@uni-jena.de

Communicated by: D. Alexandrov

## Funding information

Russian Science Foundation,  
Grant/Award Number: 21-79-10012

This paper is devoted to the mathematical modeling of a combined effect of directional and bulk crystallization in a phase transition layer with allowance for nucleation and evolution of newly born particles. We consider two models with and without fluctuations in crystal growth velocities, which are analytically solved using the saddle-point technique. The particle-size distribution function, solid-phase fraction in a supercooled two-phase layer, its thickness and permeability, solidification velocity, and desupercooling kinetics are defined. This solution enables us to characterize the mushy layer composition. We show that the region adjacent to the liquid phase is almost free of crystals and has a constant temperature gradient. Crystals undergo intense growth leading to fast mushy layer desupercooling in the middle of a two-phase region. The mushy region adjacent to the solid material is filled with the growing solid-phase structures and is almost desupercooled.

## KEYWORDS

crystal growth, heat and mass transfer, mushy layer, nucleation, phase transitions

## MSC CLASSIFICATION

80A19; 80A22

## 1 | INTRODUCTION

Directional and bulk solidification phenomena are at the basis of many technological processes for obtaining materials with given properties.<sup>1–5</sup> One of the central tasks of phase transformation is to determine the influence of external parameters (temperature gradients, supercooling, heat flow, etc.) on the microstructure and phase composition of the solidified material. Such a problem can be solved by mathematical modeling of the real process of directional and/or bulk crystallization. Mathematical models describing such processes began to be developed several decades ago. Since the phase transformation phenomenon takes place in an extended domain, the mathematical formulation of the problem is more complex than the classical Stefan-type model.<sup>6,7</sup> Here, we must consider that the phase transition does not occur at the crystallization front but in an extended metastable layer. If the supercooling of the melt is fully compensated by the release of latent heat of the phase transition, such a model is called a quasi-equilibrium model of the two-phase region (mushy layer).<sup>8–11</sup> Methods for solving such a nonlinear directional solidification model have been developed in many previous studies.<sup>12–17</sup> If the latent heat does not fully compensate for the supercooling of the metastable liquid, the phase transformation region is supercooled. As a result, the nucleation and crystal growth processes (bulk phase transition) can

This is an open access article under the terms of the Creative Commons Attribution-NonCommercial-NoDerivs License, which permits use and distribution in any medium, provided the original work is properly cited, the use is non-commercial and no modifications or adaptations are made.

© 2021 The Authors. *Mathematical Methods in the Applied Sciences* published by John Wiley & Sons, Ltd.

occur there. Approximate methods for solving the nonlinear problem describing the bulk phase transformation have been developed in several previous studies.<sup>18–24</sup> Note that in practice, directional and bulk phase transformation often occur simultaneously in the mobile supercooled region of solidification.

The present work is devoted to the mathematical modeling of such a process described by a nonlinear integrodifferential model of the heat and mass transfer equations considering nucleation and crystal growth in the supercooled liquid. In Section 2, an approximate analytical method for solving such a model without fluctuations in the growth rates of individual crystals (first-order kinetic equation) is developed. In Section 3, a method for solving such a model with fluctuations in particle growth rates (second-order kinetic equation) is detailed. In Section 4, the results of the model solution are presented, and conclusions are formulated in Section 5.

## 2 | ANALYTICAL SOLUTION FOR DIFFUSIONLESS MODEL

In this section, we consider a combined effect of directional and bulk crystallization. In addition, we assume that crystals can nucleate and evolve in a supercooled layer without fluctuations in their growth rates.

Let's consider the steady-state crystallization process along the spatial axis  $z$  with a constant velocity  $V$ . In this case, the mushy layer that is moving into the liquid divides the purely solid and liquid phases, where  $z = 0$  corresponds to the mushy/liquid interface, and  $z = -h$  represents a free boundary between the solid and mushy interfaces, respectively.

The solutal and temperature conductivity equations<sup>8,10,12,25,26</sup> take the form

$$-V \frac{d}{dz} ((1 - \varphi)\sigma) = \frac{d}{dz} \left( D \frac{d\sigma}{dz} \right) + k\sigma V \frac{d\varphi}{dz}, \quad (1)$$

$$\frac{d}{dz} \left( \lambda \frac{d\theta}{dz} \right) - VL_V \frac{d\varphi}{dz} = 0, \quad (2)$$

where  $\varphi$  is a volume fraction of solid crystals in the mush,  $\sigma$  represents a composition of the interstitial liquid,  $D$  is the solutal diffusivity,  $k$  is the ratio of the solute concentration in the solid and liquid phases,  $\lambda$  is a thermal conductivity,  $\theta$  is the temperature distribution, and  $L_V$  is the latent heat of crystallization.

Here, the solutal diffusivity  $D$  and the thermal conductivity  $\lambda$  in the phase transition layer can be expressed as functions of  $\varphi$ :

$$D(\varphi) = D_l(1 - \varphi), \quad \lambda(\varphi) = \lambda_l(1 - \varphi) + \lambda_s\varphi, \quad (3)$$

where subscripts  $s$  and  $l$  define solid and liquid phases, respectively.<sup>12,26–29</sup>

The relaxation time of temperature field  $\tau_a = l^2/a$ , where  $l$  is a characteristic length scale, and  $a$  is the temperature diffusivity coefficient, is essentially less than the relaxation time of the diffusion field  $\tau_D = l^2/D_l$ , that is,  $\tau_a/\tau_D \sim 10^{-3} - 10^{-4}$ , so we can neglect the temperature derivative with respect to time (the right-hand side of Equation 2). The steady-state crystallization velocity is defined by the temperature gradients in the solid  $g_s$  and liquid  $g_l$  and takes the form

$$V = \frac{\lambda_s g_s - \lambda_l g_l}{L_V}. \quad (4)$$

Integrating Equation (2) and keeping in mind that  $dT/dz = g_l$  at  $\varphi = 0$ , we obtain

$$\lambda(\varphi) \frac{d\theta}{dz} - VL_V \varphi = \lambda_l g_l. \quad (5)$$

The concentration field  $\sigma$  in the phase transition layer can be defined by means of the Scheil equation in the form

$$\sigma = \frac{\sigma_0}{(1 - \varphi)^{1-k}}, \quad (6)$$

where  $\sigma_0$  represents the concentration at  $\varphi = 0$ , and  $k$  is the segregation coefficient.

The phase transition temperature  $\theta_p(\sigma)$  can be defined from the phase diagram by means of the liquidus equation<sup>12,28</sup> in the form  $\theta_p(\sigma) = \theta_p^0 - m\sigma$ , where  $m$  is the liquidus slope and  $\theta_p^0$  is the phase transition temperature of pure substance at

$\sigma = 0$ , respectively. Substitution of this expression into Equations (5) and (6) gives us the following differential equation for the supercooling  $\Delta\theta(z) = \theta_p(\sigma(z)) - \theta(z)$  in a phase transition layer:

$$-b_1 \frac{d}{dz} \Delta\theta = \frac{b_2 + \varphi}{b_3 + \varphi} + b_4 \frac{1}{(1 - \varphi)^{2-k}} \frac{d\varphi}{dz}, \quad (7)$$

$$b_1 = \frac{\lambda_s - \lambda_l}{VL_V}, \quad b_2 = \frac{\lambda_l g_l}{VL_V}, \quad b_3 = \frac{\lambda_l}{\lambda_s - \lambda_l}, \quad b_4 = (1 - k)m\sigma_0 \frac{\lambda_s - \lambda_l}{VL_V},$$

where  $\varphi = \varphi(z)$ , and the boundary conditions  $\Delta\theta(0) = \Delta\theta(-h) = 0$  take place.

For the description of the nucleation and growth processes, we will use the previously developed theory for the motionless phase transition region.<sup>30,31</sup> The kinetic equation for the distribution function  $f(t, z, r)$  takes the form<sup>32</sup>

$$\frac{\partial f}{\partial t} + \frac{\partial}{\partial r} \left( \frac{dr}{dt} f \right) = 0. \quad (8)$$

Here,  $t$  is the process time,  $r$  is the radial coordinate, and  $dr/dt$  is the crystal growth velocity

$$\frac{dr}{dt} = \frac{\beta_* \Delta\theta}{1 + \beta_* (L_V / \lambda_l) r}, \quad (9)$$

where  $\beta_*$  represents the kinetic coefficient. The boundary condition takes the form

$$\left. \frac{dr}{dt} f \right|_{r=0} = I_* \exp \left( -\frac{p}{\Delta\theta^2} \right), \quad (10)$$

where  $p$  and  $I_*$  represent positive constants.<sup>33,34</sup> The boundary condition (10) describes the flux of crystals crossing the critical nucleation barrier (here, the critical radius of nucleating particles is supposed to be zero). Moreover, the right side of the boundary condition (10) takes into account the Weber–Volmer–Frenkel–Zeldovich nucleation kinetics.<sup>35</sup> We also assume that the distribution function  $f = 0$  at  $z = 0$  (at the boundary between the phase transition layer and the liquid phase).

The volume fraction  $\varphi$  of the solid phase can be defined in terms of the particle-radius distribution function as

$$\varphi = \int_0^{\infty} \frac{4\pi}{3} r^3 f(t, z, r) dr. \quad (11)$$

In the moving frame of reference, Equations (9) and (10) can be written as

$$-(1 + qr) \frac{dr}{dz} = \frac{\beta_*}{V} \Delta\theta, \quad (12)$$

$$-\frac{\partial f}{\partial z} + \frac{\beta_*}{V} \Delta\theta \frac{\partial}{\partial r} \left( \frac{f}{1 + qr} \right) = 0, \quad (13)$$

$$f|_{r=0} = \frac{I_*}{\beta_*} \frac{1}{\Delta\theta} \exp \left( -\frac{p}{\Delta\theta^2} \right), \quad (14)$$

where  $q = \beta_* L_V / \lambda_l$ , and  $f = f(z, r)$  is independent of  $t$ .

Combining Equations (13) and (14) and  $f|_{z=0} = 0$  gives

$$f = \left( 1 + \beta_* \frac{L_V}{\lambda_l} r \right) \eta(x(z) - y(r)) H(x(z) - y(r)), \quad (15)$$

where  $H$  is the Heaviside function denoting that the size of solid particles is limited to a maximum value that corresponds to the size of nucleating crystals at the liquid/mush interface, and the following designations are entered as

$$x(z) = \frac{\beta_*}{V} \int_z^0 \Delta\theta(\xi) d\xi, \quad y(r) = \int_0^r \left(1 + \beta_* \frac{L_V}{\lambda_l} r\right) dr,$$

$$\eta(u) = \frac{I_*}{\beta_*} \frac{1}{\Delta\theta(u)} \exp\left(-\frac{p}{\Delta\theta(u)^2}\right).$$

Integrating (12) with  $r = 0$  at  $z = \zeta$ , we arrive at

$$r = (\sqrt{1 + 2q(x(z) - x(\zeta))} - 1)/q. \quad (16)$$

Equation (16) determines the radius  $r(z)$  of crystals arising at the point  $z = \zeta$  inside the mushy layer.

For the sake of simplicity, let's initially develop the theory for the single-component supercooled liquids. Thus, we introduce a new variable  $\zeta$  instead of  $r$  for any constant  $z$  using the expression  $x(\zeta) = x(z) - y(r)$ . As a consequence of this, it follows that  $\beta_* \Delta\theta(\zeta) d\zeta / V = (1 + qr) dr$ , and limits of integration  $r = 0$  and  $r = r|_{\zeta=0}$  transform to corresponding limits  $\zeta = z$  and  $\zeta = 0$  in terms of  $\zeta$ . Replacing now  $r$  by  $\zeta$  in (11) and taking into account (15) and (16), we obtain

$$\varphi(z) = \frac{4\pi I_*}{3V} \int_z^0 w(z, \zeta) \exp(pS(\zeta)) d\zeta, \quad (17)$$

where

$$w(z, \zeta) = q^{-3} (\sqrt{1 + 2q(x(z) - x(\zeta))} - 1)^3, \quad S(\zeta) = -1/\Delta\theta(\zeta)^2.$$

The analytical solution can be found using the Laplace transform method. For doing this, we specify the derivative  $\Delta\theta'(z)$  in (7) is zero and then solve the differential equation for  $\varphi(z)$  as

$$\frac{b_2 + \varphi}{b_3 + \varphi} + b_4 \frac{1}{(1 - \varphi)^{2-k}} \frac{d\varphi}{dz} = 0.$$

Consequently, we arrive at the following condition for point  $v$ , where the constitutional supercooling comes to its maximum

$$v = \Sigma(\varphi) = -\frac{b_4}{1-k} \frac{1}{(1-\varphi)^{1-k}} \left[1 + \frac{b_3 - b_2}{b_2 - 1} F\left(k - 1, 1, k; \frac{1 - \varphi}{b_2 - 1}\right)\right] + \frac{b_4}{1-k} \left[1 + \frac{b_3 - b_2}{b_2 - 1} F\left(k - 1, 1, k; \frac{1}{b_2 - 1}\right)\right], \quad (18)$$

where  $F$  is the hypergeometric function<sup>36</sup>

$$F(\alpha, \beta, \gamma; x) = 1 + \sum_{k=1}^{\infty} \frac{(\alpha)_k (\beta)_k}{(\gamma)_k} \frac{x^k}{k!}.$$

Retaining the main term of the integral asymptotic expansion (17), we obtain<sup>37,38</sup>

$$\varphi(z) = a(v) \cdot w(z, v), \quad a(v) = \frac{4\pi I_*}{3V} \sqrt{-\frac{\pi}{p} \frac{\Delta\theta^3(v)}{\Delta\theta''(v)}} \exp\left(-\frac{p}{\Delta\theta^2(v)}\right). \quad (19)$$

Equation (19) demonstrates that  $\varphi(v)$  disappears since  $w(v, v) = 0$ . As the function  $\varphi(z)$  decreases,  $\varphi(z) \approx 0$  at  $v \leq z \leq 0$ . Considering this, we obtain from (7)

$$\Delta\theta(z) = -g_l z, \quad v \leq z \leq 0. \quad (20)$$

Substituting the linear supercooling as (20) into Equation (17) at  $z = \nu$ , we can obtain  $\varphi$  at  $\nu$

$$\varphi(\nu) = \frac{4\pi I_*}{3V} \int_{\nu}^0 \left( \sqrt{\frac{1}{q^2} + \frac{g_l \beta_*}{qV}(\nu^2 - \zeta^2)} - \frac{1}{q} \right)^3 \exp\left(-\frac{p}{g_l^2 \zeta^2}\right) d\zeta. \quad (21)$$

Further, substituting  $\varphi(\nu)$  into expression (18) yields the following transcendental equation relating to the point  $\nu$  of maximum supercooling as

$$\nu = \Sigma(\varphi(\nu)). \quad (22)$$

The second derivative  $\Delta\theta''(\nu)$  in the denominator  $a(\nu)$  of (19) is zero. So, in order to remedy this, we calculate the integral of (17) again by the Laplace method in the interval  $-h \leq z \leq \nu$  for the maximum boundary point  $z = \nu^{38}$ :

$$\varphi(z) = b(\nu) \cdot w(z, \nu), \quad b(\nu) = -\frac{4\pi I_* \nu^3}{3V 2p} g_l^2 \exp\left(-\frac{p}{(g_l \nu)^2}\right).$$

Thus, the solid fraction  $\varphi(z)$  within a mushy layer takes the form

$$\varphi(z) = \begin{cases} 0 & \nu \leq z \leq 0 \\ b(\nu) \cdot w(z, \nu) & -h \leq z < \nu. \end{cases} \quad (23)$$

Now let us rewrite Equation (7) in terms of variable  $x_\nu$ :

$$x_\nu = x(z) - x(\nu) = \frac{\beta_*}{V} \int_z^\nu \Delta\theta(\xi) d\xi, \quad (24)$$

$$\frac{d}{dz} = \frac{dx_\nu}{dz} \frac{d}{dx_\nu} = -\frac{\beta_*}{V} \Delta\theta \frac{d}{dx_\nu}.$$

Consequently, we arrived at the constitutive supercooling inside the part  $-h \leq z \leq \nu$  of a mushy layer. This supercooling is governed by the equation

$$\Delta\theta(x_\nu) \cdot \Delta\theta'(x_\nu) = -c_1 \frac{1}{(1-\varphi)^{2-k}} \frac{d\varphi}{dx_\nu} \Delta\theta(x_\nu) + c_2 \frac{b_2 + \varphi}{b_3 + \varphi}, \quad (25)$$

where

$$c_1 = b_4/b_1, \quad c_2 = V/(\beta_* b_1), \quad \varphi = \varphi(x_\nu) = b w(x_\nu),$$

$$w(x_\nu) = (\sqrt{1 + 2q x_\nu} - 1)^3 / q^3.$$

It can be easily seen that  $x_\nu$  changes from 0 to a certain point  $x_h$  if we vary  $z$  from  $\nu$  to  $-h$ . Substituting  $z = \nu$  (or  $x_\nu = 0$ ) into (20), we obtain the boundary condition  $\Delta\theta(0) = -g_l \nu$ . Therefore, the moving boundary problem is reduced to a first-order differential equation (25) for constitutional supercooling, augmented by the boundary condition (the standard Cauchy problem for the Abelian equation). This equation can be solved numerically.

The mushy layer thickness  $h$  can be found by equating the liquidus and boundary temperatures that follows  $\Delta\theta(x_h) = 0$ . Substituting this condition into Equation (25) leads to the expression  $(b_2 + \varphi)/(b_3 + \varphi) = 0$ . To overcome the difficulty connected with thermophysical parameters  $\varphi \geq 0$ ,  $b_2 > 0$ , and  $b_3 > 0$ , we take  $\varphi = 1$  at  $x_\nu = x_h$ . In this case,  $x_h$  is easily defined by eq.  $b w(x_h) = 1$ , from which it follows that

$$x_h = \frac{1}{2q} ((b^{-3}q + 1)^2 - 1).$$

The spatial coordinate  $z$  as a function of  $x_v$  can be written as

$$z = z(x_v) = v - \frac{V}{\beta_*} \int_0^{x_v} \frac{d\xi}{\Delta\theta(\xi)}. \quad (26)$$

### 3 | ANALYTICAL SOLUTION FOR DIFFUSIONAL MODEL

In this section, possible fluctuations in crystal growth rates are taken into account using the second-order differential kinetic equation for the particle-radius distribution function.<sup>32</sup> To describe the nucleation and growth processes, we will use the previously developed approach for the motionless phase transition region.<sup>39–41</sup> This approach considers the diffusive mechanism of the crystal size distribution function in the crystal radius space and the nonstationary growth velocities of individual particles caused by external fluctuations. In this case, the kinetic equation (8) for the distribution function  $f$  takes the form<sup>32</sup>

$$\frac{\partial f}{\partial t} + \frac{\partial}{\partial r} \left( \frac{dr}{dt} f \right) = \frac{\partial}{\partial r} \left( D \frac{\partial f}{\partial r} \right), \quad (27)$$

where  $D = d_1 dr/dt$ ,  $d_1$  is a pertinent factor.

Combining Equations (10), (11), and (27), we arrive at the following boundary-value problem in a moving reference frame

$$\frac{\partial f}{\partial s} + \frac{\partial f}{\partial r} = d_1 \frac{\partial^2 f}{\partial r^2}, \quad r > 0, s > 0, \quad (28)$$

$$f - d_1 \frac{\partial f}{\partial r} = \frac{I_* \exp[-p/(\Delta\theta)^2]}{\beta_* \Delta\theta} = J(s), \quad r = 0, \quad (29)$$

$$f \rightarrow 0, \quad r \rightarrow \infty; \quad f = 0, \quad s = 0, \quad (30)$$

where

$$s = -\frac{\beta_*}{V} \int_0^z \Delta\theta(z_1) dz_1. \quad (31)$$

The analytical solution of Equations (28)–(30) may be obtained by the Laplace transform method and has the form<sup>33,42</sup>

$$f = \int_0^s J(s - s_1) \gamma(r, s_1) ds_1, \quad (32)$$

$$\begin{aligned} \gamma(r, s_1) = & \frac{1}{2d_1} \exp\left(\frac{2r - s_1}{4d_1}\right) \left[ \frac{2\sqrt{d_1}}{\sqrt{\pi s_1}} \exp\left(-\frac{r^2}{4d_1 s_1}\right) \right. \\ & \left. - \exp\left(\frac{r}{2d_1} + \frac{s_1}{4d_1}\right) \operatorname{erfc}\left(\frac{r}{2\sqrt{d_1 s_1}} + \frac{\sqrt{s_1}}{2\sqrt{d_1}}\right) \right], \end{aligned}$$

where  $J(s - s_1)$  is determined by expression (29).

Substituting  $f$  from (32) into (11) and evaluating the integral over  $r$ , we obtain the solid fraction as

$$\varphi(s) = \frac{4\pi}{3} \int_0^s J(s - s_1) R(s_1) ds_1, \quad (33)$$

$$R(s_1) = \frac{\exp(-s_1/(4d_1))}{\sqrt{\pi}} \left[ \frac{b(s_1)}{2} - 2d_1^{1/2} s_1^{5/2} - 3d_1^{3/2} s_1^{3/2} \right]$$

$$-\left(\frac{c(s_1)}{2} + 3d_1^3\right) \operatorname{erfc}\left(\frac{\sqrt{s_1}}{2\sqrt{d_1}}\right) + c(s_1),$$

$$b(s_1) = 20d_1^{3/2}s_1^{3/2} + 6d_1^{1/2}s_1^{5/2} - 12d_1^{5/2}s_1^{1/2},$$

$$c(s_1) = 9d_1s_1^2 + s_1^3 + 6d_1^3.$$

Substituting  $J$  from (29) into (33) and replacing the integration variable, we obtain

$$\varphi(s) = \frac{4\pi I_*}{3\beta_*} \int_0^s \frac{\exp[pS(s_2)]}{\Delta\theta(s_2)} R(s-s_2) ds_2, \quad (34)$$

where  $S(s_2) = -[\Delta\theta(s_2)]^{-2}$ . This integral can be evaluated using the saddle-point method.<sup>38</sup> With only the main term of the asymptotic expansion in mind, we obtain

$$\varphi(s) \approx \frac{4\pi I_*}{3\beta_*} \frac{\exp[pS(\nu)]}{\Delta\theta(\nu)} R(s-\nu) \sqrt{-\frac{\pi[\Delta\theta(\nu)]^3}{p[\Delta\theta(\nu)]''}}, \quad (35)$$

where  $\nu$  is the point of extremum of the function  $S(s_2)$ , which coincides with the maximum point of supercooling  $\Delta\theta(s_2)$ . Considering this, from Equation (7), we have

$$z_\nu = -b_4 \int_0^{\varphi_\nu} \frac{(b_3 + \tilde{\varphi}) d\tilde{\varphi}}{(1 - \tilde{\varphi})^{2-k} (b_2 + \tilde{\varphi})}, \quad (36)$$

where subscript  $\nu$  designates the maximum point.

The analytical solution (35) demonstrates that  $\varphi(\nu) \approx 0$  due to the fact that  $R(0) = 0$ . With this in mind, we obtain from Equation (7)

$$\Delta\theta = -g_l z, \quad z_\nu \leq z \leq 0. \quad (37)$$

Combining expressions (31) and (37), we come to

$$\nu = \frac{\beta_* g_l x_\nu^2}{2V}, \quad s = \frac{\beta_* g_l z^2}{2V}, \quad z_\nu \leq z \leq 0. \quad (38)$$

Substituting  $\Delta\theta$  from (37) into (35), we can find the solid fraction in the form

$$\varphi_\nu = \frac{4\pi I_*}{3\sqrt{2V}\beta_* g_l} \int_0^\nu \frac{\exp[-p\beta_*/(2Vg_l s_2)] R(\nu-s_2) ds_2}{\sqrt{s_2}}. \quad (39)$$

Calculating the integral (34) by the saddle-point method in the region  $-h \leq z < z_\nu$ , we now arrive at the final distribution of the solid-phase fraction as

$$\varphi(s) \approx \begin{cases} \frac{2\pi I_* \exp[-p/(g_l x_\nu)^2] g_l x_\nu^2 R(s-\nu)}{3p\beta_*}, & -h \leq z < z_\nu, \\ 0, & z_\nu \leq z \leq 0 \end{cases}, \quad (40)$$

where the solid-phase fraction becomes zero at  $s = \nu$  ( $z = z_\nu$ ).

Considering that

$$dz = -\frac{V}{\beta_* \Delta\theta} ds, \quad (41)$$

we obtain from (7) the standard Cauchy problem that defines the supercooling in the region  $-h \leq z < z_v$

$$\frac{d\Delta\theta}{ds} = \frac{V}{b_1 \beta_* \Delta\theta} \left[ \frac{b_2 + \varphi}{b_3 + \varphi} - \frac{b_4 \beta_* \Delta\theta}{V(1-\varphi)^{2-k}} \frac{d\varphi}{ds} \right], \quad (42)$$

$$\Delta\theta = -g_l z_v, \quad s = v$$

where  $d\varphi/ds$  is defined from Equation (40). Note that the left boundary  $z = -h$  of the phase transition layer is determined from the boundary condition  $\Delta\theta = 0$  at  $z = -h$ . In addition, the parametric dependence between  $z$  and  $s$  can be obtained from (41) and takes the form

$$z = -\frac{V}{\beta_*} \int_v^s \frac{ds_1}{\Delta\theta(s_1)} + z_v. \quad (43)$$

## 4 | DISCUSSION

In this section, we discuss the analytical solutions obtained in Sections 2 and 3 for the diffusionless and diffusional models. First of all, Figure 1 demonstrates the supercooling and solid-phase fraction profiles within the mushy layer. As is easily seen, the two-phase region is formally divided into three sublayers. The first layer adjacent to the liquid material contains a small number of solid particles ( $\varphi \approx 0$ ) and has a linear distribution of the supercooling  $\Delta\theta$ . The second intermediate layer (to the left of the first one) contains a substantial quantity of the solid phase, which grows, releases the latent heat, and partially compensates the mushy layer supercooling. In the third layer, which is adjacent to the solid material, the melt supercooling is almost zero, and the solid phase evolves in a quasi-equilibrium manner completely compensating  $\Delta\theta$ . An important point is that both models (diffusionless and diffusional) demonstrate a very similar behavior of  $\Delta\theta(z)$  and  $\varphi(z)$ .

The known solid-phase profile in the two-phase layer enables us to find the mushy layer permeability  $\Pi(\varphi)$ ,<sup>43–45</sup> which determines material microstructure

$$\Pi(\varphi) = (1 - \varphi)^3. \quad (44)$$

Its profile in the mushy region is illustrated in Figure 2 for the diffusional model. As is seen,  $\Pi(\varphi) \approx 1$  at the mushy layer–liquid-phase boundary where  $\varphi \approx 0$ . In addition,  $\Pi(\varphi)$  decreases in a nonlinear manner with increasing  $\varphi$  and decreasing  $z$  when approaching the mushy layer–solid-phase boundary.

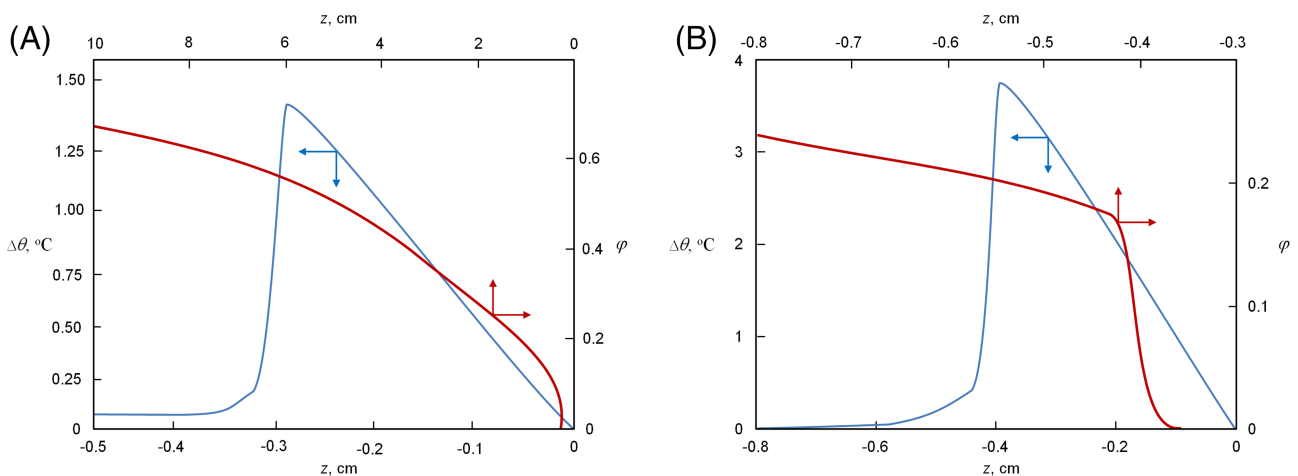


**FIGURE 1** The mushy layer supercooling  $\Delta\theta$  (scale of values on the left) and the solid-phase fraction  $\varphi$  (scale of values on the right) as functions of the spatial coordinate  $z$ . (A) and (B) respectively correspond to the diffusionless and diffusional models. Parameters used in calculations are  $b_1 = 0.2 \text{ cm} (\text{°C})^{-1}$ ,  $b_2 = 2$ ,  $b_3 = 2$ ,  $b_4 = 5.4 \text{ cm}$ ,  $k = 0.1$ ,  $q = 5 \cdot 10^4 \text{ cm}^{-1}$ ,  $p = 10 (\text{°C})^2$ ,  $\beta_*/V = 2 \cdot 10^4 (\text{°C})^{-1}$ , and  $I_*/V = 2 \cdot 10^4 \text{ cm}^{-4}$  [Colour figure can be viewed at [wileyonlinelibrary.com](http://wileyonlinelibrary.com)]



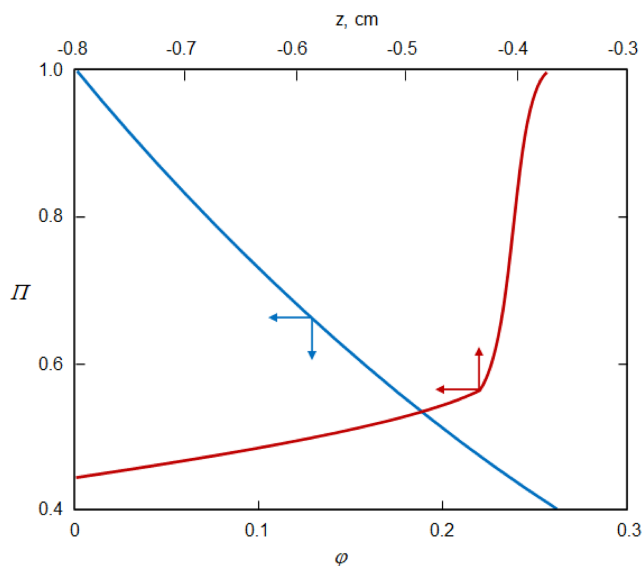


**FIGURE 2** The mushy layer permeability as a function of the solid-phase fraction  $\phi$  and spatial coordinate  $z$  in the mushy region [Colour figure can be viewed at [wileyonlinelibrary.com](http://wileyonlinelibrary.com)]

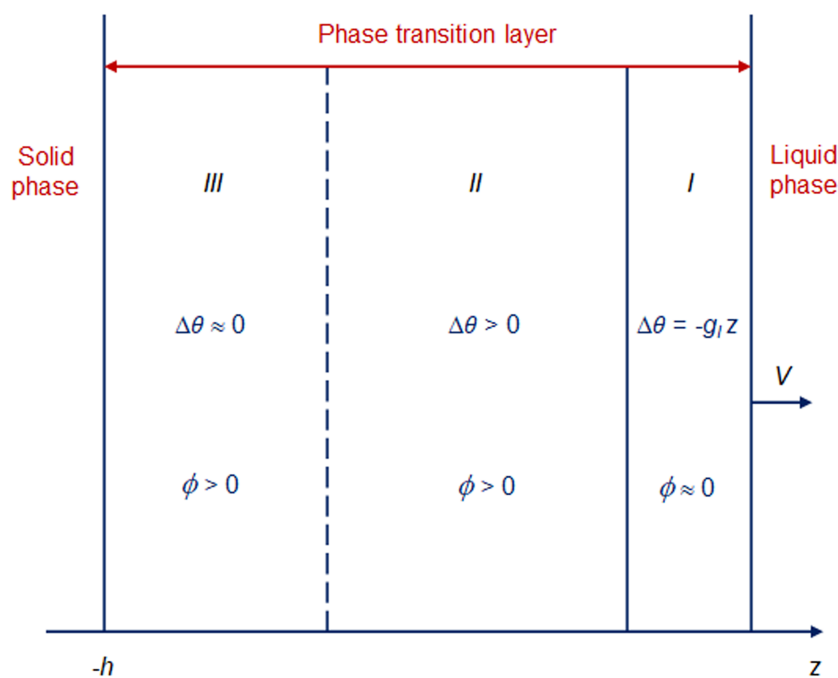


**FIGURE 3** Illustration of the moving phase transition layer, which contains three sublayers: *I*, *II*, and *III* [Colour figure can be viewed at [wileyonlinelibrary.com](http://wileyonlinelibrary.com)]

The mushy region structure is summarized in Figure 3, where three aforementioned sublayers, *I*, *II*, and *III*, are illustrated schematically. The analytical theory under consideration shows that the bulk phase transition predominantly occurs in the middle region *II*, while the directional phase transformation primarily goes in the left sublayer *III*.

## 5 | CONCLUSION

In this paper, the problem of synchronous operation of the directional and bulk phase transitions in metastable liquids is analyzed theoretically. Here, we develop two integrodifferential models with moving boundaries of the phase transition. One of them includes the so-called “diffusion” mechanism of particles in the space of their sizes (the second-order kinetic equation), whereas the second one neglects this mechanism (the first-order kinetic equation). Both models are solved analytically using the saddle-point technique for the evaluation of Laplace-type integrals. As a result, the temperature field, melt supercooling, solid-phase distribution, and permeability of the two-phase layer as well as its moving boundaries are analytically defined. Our solution demonstrates the complex mushy layer structure responsible for its properties and material microstructure. The main conclusion is that particles nucleate and evolve mainly in the middle sublayer of

a mush (bulk phase transformation). In addition, the solid phase in the form of dendrite-like structures grows primarily in the region adjacent to the solid material (directional phase transformation). Another sublayer adjacent to the liquid phase is almost free of solid-phase particles and structures. In this region, the temperature behaves as a linear function of the spatial coordinate  $z$ . Another important circumstance is that the middle sublayer is mainly responsible for the desupercooling. This is due to the fact of intense nucleation of solid-phase crystals, which release the latent heat of solidification and thus compensate for the melt supercooling. On the other hand, the region adjacent to the solid phase is in the quasi-equilibrium state; that is, its supercooling is almost compensated by the latent heat.

The theory under consideration opens ways for further investigation of the joint realization of bulk and directional phase transformation. For example, an important task is to analyze the morphological and dynamic stability of the two-phase region, which can be carried out in the spirit of previous studies.<sup>46–48</sup> Another important task is to study unsteady crystallization scenario of simultaneous bulk and directional crystallization, which can be developed accordingly to the previous solidification theory with a mushy layer.<sup>14–16</sup>

## ACKNOWLEDGEMENT

The authors gratefully acknowledge financial support from the Russian Science Foundation (project no. 21-79-10012). Open Access funding enabled and organized by Projekt DEAL.

## AUTHOR CONTRIBUTIONS

The authors contributed equally to the present research article.

## CONFLICT OF INTERESTS

The authors declare no potential conflicts of interest.

## ORCID

Liubov V. Toropova  <https://orcid.org/0000-0003-4587-2630>

Danil L. Aseev  <https://orcid.org/0000-0001-5894-8126>

Alexander A. Ivanov  <https://orcid.org/0000-0002-2490-160X>

## REFERENCES

1. Chalmers B. *Principles of Solidification*. New York: Wiley; 1964.
2. Kurz W, Fisher DJ. *Fundamentals of Solidification*. Aedermannsdorf: Trans. Tech. Publ.; 1989.
3. Herlach D, Galenko P, Holland-Moritz D. *Metastable Solids from Undercooled Melts*. Amsterdam: Elsevier; 2007.
4. Galenko PK, Alexandrov DV. From atomistic interfaces to dendritic patterns. *Phil Trans R Soc A*. 2018;376:20170210.
5. Alexandrov DV, Zubarev AY. Patterns in soft and biological matters. *Phil Trans R Soc A*. 2020;378:20200002.
6. Gupta SC. *Classical Stefan Problem*. Amsterdam: Elsevier; 2003.
7. Alexandrova IV, Alexandrov DV, Aseev DL, Bulitcheva SV. Mushy layer formation during solidification of binary alloys from a cooled wall: the role of boundary conditions. *Acta Phys Pol A*. 2009;115:791-794.
8. Hills RN, Loper DE, Roberts PH. A thermodynamically consistent model of a mushy zone. *Q J Appl Maths*. 1983;36:505-539.
9. Fowler AC. The formation of freckles in binary alloys. *IMA J Appl Math*. 1985;35:159-174.
10. Borisov VT. *Theory of Two-Phase Zone of a Metal Ingot*. Moscow: Metallurgiya Publishing House; 1987.
11. Alexandrov DV. Solidification with a quasiequilibrium two-phase zone. *Acta Mater*. 2001;49:759-764.
12. Worster MG. Solidification of an alloy from a cooled boundary. *J Fluid Mech*. 1986;167:481-501.
13. Aseev DL, Alexandrov DV. Unidirectional solidification with a mushy layer. The influence of weak convection. *Acta Mater*. 2006;54:2401-2406.
14. Alexandrov DV, Malygin AP. Analytical description of seawater crystallization in ice fissures and their influence on heat exchange between the ocean and the atmosphere. *Dokl Earth Sci*. 2006;411:1407-1411.
15. Alexandrov DV, Aseev DL, Nizovtseva IG, Huang H-N, Lee D. Nonlinear dynamics of directional solidification with a mushy layer. Analytic solutions of the problem. *Int J Heat Mass Trans*. 2007;50:3616-3623.
16. Alexandrov DV, Nizovtseva IG, Malygin AP, Huang H-N, Lee D. Unidirectional solidification of binary melts from a cooled boundary: analytical solutions of a nonlinear diffusion-limited problem. *J Phys Condens Matter*. 2008;20:114105.
17. Alexandrov DV, Ivanov AA. Solidification of a ternary melt from a cooled boundary, or nonlinear dynamics of mushy layers. *Int J Heat Mass Trans*. 2009;52:4807-4811.

18. Buyevich YA, Mansurov VV. Kinetics of the intermediate stage of phase transition in batch crystallization. *J Cryst Growth*. 1990;104:861-867.
19. Buyevich YA, Mansurov VV, Natalukha IA. Instability and unsteady processes of the bulk continuous crystallization—I. Linear stability analysis. *Chem Eng Sci*. 1991;46:2573-2578.
20. Makoveeva EV, Alexandrov DV. Effects of nonlinear growth rates of spherical crystals and their withdrawal rate from a crystallizer on the particle-size distribution function. *Phil Trans R Soc A*. 2019;377:20180210.
21. Ivanov AA, Alexandrova IV, Alexandrov DV. Phase transformations in metastable liquids combined with polymerization. *Phil Trans R Soc A*. 2019;377:20180215.
22. Alexandrov DV, Nizovtseva IG, Alexandrova IV. On the theory of nucleation and nonstationary evolution of a polydisperse ensemble of crystals. *Int J Heat Mass Trans*. 2019;128:46-53.
23. Alexandrova IV, Alexandrov DV. Dynamics of particulate assemblages in metastable liquids: a test of theory with nucleation and growth kinetics. *Phil Trans R Soc A*. 2020;378:20190245.
24. Nikishina MA, Alexandrov DV. Nucleation and growth dynamics of ellipsoidal crystals in metastable liquids. *Phil Trans R Soc A*. 2021;379:20200306.
25. Buyevich YA, Alexandrov DV, Mansurov VV. *Macrokinetics of Crystallization*. New York: Begell House; 2001.
26. Buyevich YA, Alexandrov DV. *Heat Transfer in Dispersions*. New York: Begell House; 2005.
27. Batchelor GK. Transport properties of two-phase materials with random structure. *Annu Rev Fluid Mech*. 1974;6:227-255.
28. Huppert EH, Worster MG. Dynamic solidification of a binary melt. *Nature*. 1985;314:703-707.
29. Kerr RC, Woods AW, Worster MG, Huppert HE. Solidification of an alloy cooled from above. Part 1. Equilibrium growth. *J Fluid Mech*. 1990;216:323-342.
30. Alexandrov DV. Nonlinear dynamics of polydisperse assemblages of particles evolving in metastable media. *Eur Phys J Special Topics*. 2020;229:383-404.
31. Makoveeva EV, Alexandrov DV. An analytical solution to the nonlinear evolutionary equations for nucleation and growth of particles. *Phil Mag Lett*. 2018;98:199-208.
32. Lifshitz EM, Pitaevskii LP. *Physical Kinetics*. Oxford, UK: Pergamon; 1981.
33. Alexandrov DV. On the theory of transient nucleation at the intermediate stage of phase transitions. *Phys Lett A*. 2014;378:1501-1504.
34. Alexandrov DV, Nizovtseva IG. On the theory of crystal growth in metastable systems with biomedical applications: protein and insulin crystallization. *Phil Trans R Soc A*. 2019;377:20180214.
35. Alexandrov DV, Malygin AP. Transient nucleation kinetics of crystal growth at the intermediate stage of bulk phase transitions. *J Phys A Math Theor*. 2013;46:455101.
36. Polyanin AD, Zaytsev VF. *Handbook of Exact Solutions for Ordinary Differential Equations*. New York: CRC Press; 2001.
37. Nayfen AH. *Introduction to Perturbation Techniques*. New York: Wiley; 1981.
38. Fedoryuk MV. *Asymptotics: Integrals and Series*. Moscow: Nauka Publishing House; 1987.
39. Alexandrov DV, Makoveeva EV. The Gibbs-Thomson effect in the evolution of particulate assemblages in a metastable liquid. *Phil Lett A*. 2020;384:126259.
40. Makoveeva EV, Alexandrov DV. How the shift in the phase transition temperature influences the evolution of crystals during the intermediate stage of phase transformations. *Eur Phys J Special Topics*. 2020;229:2923-2935.
41. Makoveeva EV, Alexandrov DV. The influence of non-stationarity and interphase curvature on the growth dynamics of spherical crystals in a metastable liquid. *Phil Trans R Soc A*. 2021;379:20200307.
42. Alexandrov DV. Nucleation and crystal growth in binary systems. *J Phys A Math Theor*. 2014;47:125102.
43. Amberg D, Homsy GM. Nonlinear analysis of buoyant convection in binary solidification with application to channel formation. *J Fluid Mech*. 1993;252:79-98.
44. Schulze TP, Worster MG. A numerical investigation of steady TP convection in mushy layers during the directional solidification of binary alloys. *J Fluid Mech*. 1998;356:199-220.
45. Schulze TP, Worster MG. Weak convection, liquid inclusions and the formation of chimneys in mushy layers. *J Fluid Mech*. 1999;388:197-215.
46. Mullins WW, Sekerka RF. Stability of a planar interface during solidification of a dilute binary alloy. *J Appl Phys*. 1964;35:444-451.
47. Alexandrov DV, Ivanov AA. Dynamic stability analysis of the solidification of binary melts in the presence of a mushy region: changeover of instability. *J Cryst Growth*. 2000;210:797-810.
48. Alexandrov DV, Malygin AP. Flow-induced morphological instability and solidification with the slurry and mushy layers in the presence of convection. *Int J Heat Mass Trans*. 2012;55:3196-3204.

**How to cite this article:** Toropova LV, Aseev DL, Osipov SI, Ivanov AA. Mathematical modeling of bulk and directional crystallization with the moving phase transition layer. *Math Meth Appl Sci*. 2022;45(13): 8011-8021. <https://doi.org/10.1002/mma.7864>